A Mechanism of Anomalous Diffusion in Particle Beams

D. Jeon,[1] M. Ball,[1] J. Budnick,[1] C. M. Chu,[1] M. Ellison,[1] B. Hamilton,[1] X. Kang,[1] L. L. Kiang,[1] S. Y. Lee,[1] K. Y. Ng,[2] A. Pei,[1] A. Riabko,[1] T. Sloan,[1] and M. Syphers[3]
[1]*Department of Physics, Indiana University, Bloomington, Indiana 47405*
[2]*Fermilab, P.O. Box 500, Batavia, Illinois 60510*
[3]*AGS Department, Brookhaven National Laboratory, Upton, New York 11973*
(Received 2 September 1997)

Experimental observation of particle diffusion mechanism in the presence of overlapping parametric resonances generated by a time dependent rf phase modulation is analyzed. We find that the regime of fast emittance growth is associated with the rapid particle motion along the separatrix of a dominant parametric resonance, the slow growth regime is related to particle diffusion in the chaotic sea, and the emittance saturation occurs when beam particles fill the chaotic region bounded by an invariant torus. Experimental data observed at the Indiana University Cyclotron Facility (IUCF) Cooler Ring are shown to agree well with the theoretical analysis. [S0031-9007(98)05562-8]

PACS numbers: 29.27.Bd, 05.45.+b, 41.75.–i

Sources of random noise such as the quantum fluctuation, Schottky signal, intrabeam scattering, etc., play an important role in beam physics. These random noise sources can usually be represented by the Langevin force in the equation of motion. When particles are acted on by the Langevin force, they diffuse in phase space. Applying the central limit theorem for the random statistically independent noise, the mean square width of the beam distribution satisfies the Einstein relation: $\sigma^2 \approx \mathcal{D}t$, where $\mathcal{D}$ is the diffusion coefficient. However, there are many diffusion processes where the Einstein relation may not be satisfied. The diffusion process of these systems is usually called *anomalous diffusion* [1]. Examples of anomalous diffusion can be found in plasma physics, Lévy dynamics, turbulent flow, space charge dominated beams [2], etc. The source and the mechanism of the anomalous diffusion have been of considerable interest in physics in recent years.

In particle beam physics, controlled particle diffusion has many applications. Some of these applications are controlled beam dilution, stochastic beam scraping, stochastic slow beam extraction, etc. For example, a secondary high frequency rf system has been employed for controlled longitudinal beam emittance dilution [3], which can minimize the negative mass instability across the transition energy [4]. The procedure is to modulate the phase of a secondary rf system. The phase modulation can lead to a controlled beam dilution before the transition energy crossing. Earlier theoretical studies indicated that the diffusion mechanism is dominated by a single parametric resonance [3]. However, a single parametric resonance can hardly lead to a uniformly distributed final beam bunch that is usually observed experimentally [5]. In order to further understand the particle diffusion mechanism, we performed several beam physics experiments at the Indiana University Cyclotron Facility (IUCF) Cooler Ring.

The series of experiments at the IUCF Cooler Ring employed a primary rf system operating at the harmonic number $h_1 = 1$ and a secondary rf system at $h_2 = 9$. The experimental procedure was as follows: Protons at 45 MeV kinetic energy were injected into the Cooler Ring with only a primary rf system operating at the harmonic number $h_1 = 1$ with rf frequency $f_0 = 1.031\,68$ MHz. The voltage of the primary rf system was $V_1 = 269$ V, and the corresponding synchrotron frequency was 667 Hz. The beam was cooled using electron cooling for 3 s. The phase space damping time of the longitudinal cooling at the IUCF Cooler was typically 0.1–0.4 s. The equilibrium bunch length was about 12 ± 1 ns. To study the particle diffusion process, a secondary rf cavity was turned on with rf phase modulation after 3 s from the injection. The rf phase modulation hardware has been calibrated to within about 5% and has been previously published [6]. The evolution of the beam profile was measured with a high bandwidth beam position monitor through a low loss high bandwidth cable. The beam profile was digitized by a digital scope with 512 channels, where each channel had a resolution of 1 ns.

In the absence of the secondary rf system, the synchrotron motion is given by

$$\dot{\delta} = -\nu_s \sin\phi - \lambda\delta + D\xi(\theta), \tag{1}$$

$$\dot{\phi} = \nu_s \delta, \tag{2}$$

where the overdot corresponds to the derivative with respect to the orbital angle θ, λ is the damping decrement, $\nu_s = (\frac{h_1 e V_1 |\eta|}{2\pi\beta^2 E})^{1/2}$ is the small amplitude synchrotron tune of the primary rf cavity system, and $[\phi, \delta]$ are, respectively, the phase of a particle relative to that of the synchronous particle and the normalized fractional momentum error $\delta = -\frac{h|\eta|}{\nu_s}\frac{\Delta p}{p_0}$, and η is the phase slip factor. The white Gaussian noise function $\xi(\theta)$ satisfies

$$\langle \xi(\theta)\xi(\theta')\rangle = \delta(\theta - \theta'), \qquad \langle \xi(\theta)\rangle = 0,$$

where $\langle \cdots \rangle$ means ensemble average, and D is the amplitude of the intrinsic white noise that may arise from beam-gas scattering, intrabeam scattering, and other noises in

 0031-9007/98/80(11)/2314(4)$15.00

storage rings. The corresponding diffusion coefficient is $\mathcal{D} = D^2/2$. The equilibrium particle distribution function that satisfies the Fokker-Planck-Vlasov equation of the stochastic dynamical system with white noise is given by [7]

$$\rho(\phi, \delta) = \frac{1}{\mathcal{N}} e^{-H_0/E_{\rm th}}, \tag{3}$$

where $H_0 = \frac{1}{2}\nu_s \delta^2 + \nu_s(1 - \cos\phi)$ is the unperturbed Hamiltonian, $\mathcal{N}$ is the normalization constant, and $E_{\rm th} = \frac{D^2}{2\lambda}$ is the "thermal energy" of the beam. In the small bunch approximation, we have $\sigma_\phi = \sqrt{E_{\rm th}}$. At the IUCF Cooler Ring, we had typically $\lambda \approx 3 \times 10^{-6}$, and $D \approx 2 \times 10^{-4}$, and the equilibrium bunch length was 12 ns at our operational condition.

When the secondary rf modulational system is turned on, the corresponding equations of motion become [8]

$$\dot{\delta} = -\nu_s[\sin\phi - r\sin(h\phi + \Delta\phi)] - \lambda\delta + D\xi(\theta), \tag{4}$$

$$\dot{\phi} = \nu_s \delta, \tag{5}$$

where $r = V_2/V_1$ is the ratio of the primary and secondary rf voltages, $h = h_2/h_1$ is the ratio of harmonic numbers, and V_1 (V_2) and h_1 (h_2) are, respectively, the voltage and harmonic number for the primary (secondary) rf system. The phase of the secondary rf cavity is modulated by

$$\Delta\phi(t) = A\sin(\nu_{\rm m}\theta + \alpha) + \Delta\phi_0,$$

where A is the modulation amplitude, α is the arbitrary phase of the secondary rf phase modulation, $\nu_{\rm m} = f_{\rm m}/f_0$ is the modulation tune, and $\Delta\phi_0$ is the relative phase difference between the two rf systems.

Figure 1 shows an example of the observed mountain range plot that displays the evolution of the beam profile for a modulation frequency $f_{\rm m} = 1400$ Hz, modulation amplitude $A = 100°$, and a voltage ratio $r = 0.11$. The evolution of the beam profile can be characterized by the rms bunch length σ^2 defined as

$$\sigma^2 = \frac{1}{N}\sum_{i=1}^{N}(\phi_i - \phi_{\rm avg})^2, \tag{6}$$

where N is the number of particles in a beam bunch, ϕ_i is the phase coordinate of the ith particle, and $\phi_{\rm avg} = \frac{1}{N}\sum_{i=1}^{N}\phi_i$ is the average phase of the beam. Figure 2 shows the evolution of σ_t^2 (in ns^2) vs the time t (in μs) of the data shown in Fig. 1. The characteristic feature of the bunch diffusion shows that the rms bunch length oscillates widely, and damps eventually into an rms value with a smaller oscillation amplitude. On the other hand, Fig. 3 shows two examples of similar particle diffusion experimental data where the rms bunch lengths exhibit a smooth diffusion of linear or nonlinear growth and reach a saturation after about 10 ms. What causes different behavior of the particle diffusion mechanism?

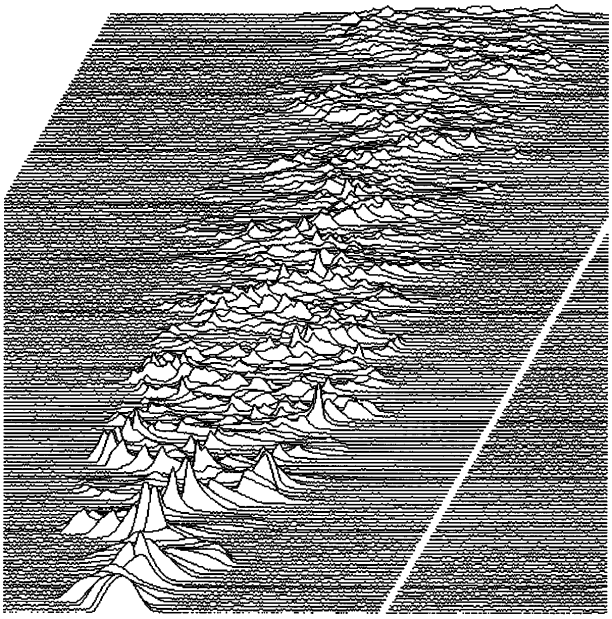

FIG. 1. The mountain range plot of the evolution of the beam profile under the action of a modulational secondary rf system, where $r = 0.11$, $f_{\rm m} = 1400$ Hz, and $A = 100°$. The horizontal axis is the bunch length of a total of 512 channels with 1 ns resolution; the total number of profile traces were 1024 in about 25 ms.

Can one identify the diffusion mechanism with underlying stochasticity in the dynamical system? What role do overlapping parametric resonances play in the diffusion process?

Neglecting the intrinsic diffusion term D and phase space damping term λ, the equations of motion can be cast into a Hamiltonian given by

$$H = \frac{1}{2}\nu_s\delta^2 + \nu_s\left[(1 - \cos\phi) - \frac{r}{h}(1 - \cos[h\phi + \Delta\phi])\right]. \tag{7}$$

The Hamiltonian can be divided into a time independent term $\langle H\rangle$ and a time dependent perturbation $H_1 = H - \langle H\rangle$. Strong perturbation to particle motion occurs only when parametric resonances are excited by the time dependent term [8,9]. The locations of the parametric resonances in the phase space are essentially determined by the Hamiltonian system. Since the "equivalent time independent" Hamiltonian of Eq. (7) depends on the parameter $\Delta\phi_0$, the final beam distribution depends sensitively on the relative phase $\Delta\phi_0$. Figure 4 shows σ_t^2 vs time, obtained from numerical simulation of 4000 particles, for $\Delta\phi_0 = 180°$ and $245°$, respectively. The sensitivity of the beam diffusion process on the $\Delta\phi_0$ parameter can be understood easily by viewing the Poincaré surfaces of section of these two dynamical systems shown in the lower plots of Fig. 5. Because the initial beam distribution occupies only

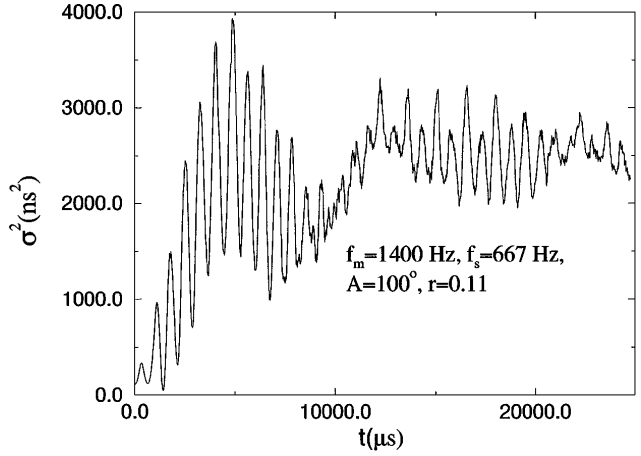

FIG. 2. Data of σ^2 (ns^2) obtained from the observed profile data shown in Fig. 1 for $f_{\rm m} = 1400$ Hz, $A = 100°$, $r = 0.11$, and $h = 9$.

a very small area in the phase space, the final beam distribution depends on the actual chaotic region that overlaps with the initial phase space. The beam will evolve into a final distribution as shown in the upper plots bounded by invariant tori. The topology of chaotic region depends sensitively on the parameters $\Delta\phi_0$ and $f_{\rm m}$.

Now, we would like to understand the significance of the large amplitude oscillation in the rms beam width σ_t^2 observed in Fig. 2. Figure 6 shows the evolution of the phase space distribution due to the secondary rf phase modulation, where the first frame corresponds to the initial phase space distribution, and a time lapse of 2.92 ms in each succeeding frame. The large amplitude oscillation shown in Fig. 2 arises from the forced oscillation similar to that of frame 2 in Fig. 6. The period of each oscillation shown in Fig. 4 corresponds to the period of coherent synchrotron motion, i.e., half the modulation period in this case. The maximum σ_t^2 corresponds to the time that particles diffuse into the maximum extent of the dominant parametric resonance. As particles gradually fill the

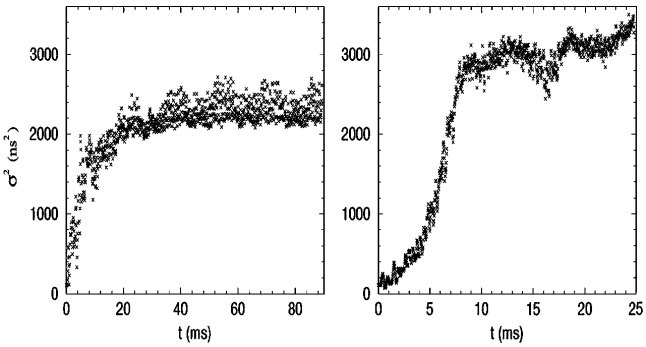

FIG. 3. Data of σ^2 (ns^2) for $A = 50°$, $r = 0.2$, and $f_{\rm m} = 1100$ Hz (left) and 2700 Hz (right), respectively. The evolution of the rms bunch lengths differs from that of Fig. 2. The left plot shows a characteristic linear growth of σ_t^2, while the right plot shows a characteristic anomalous diffusion.

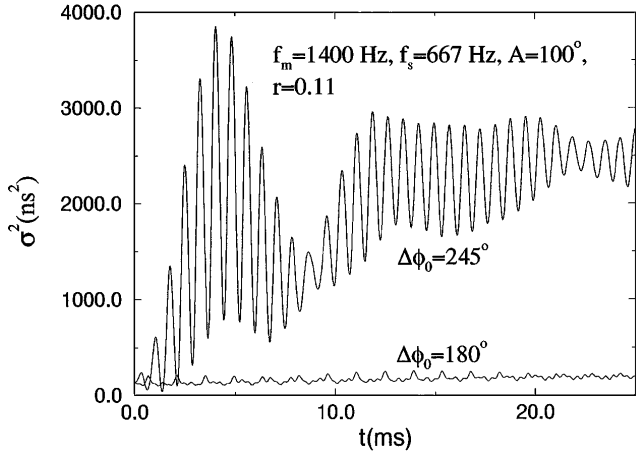

FIG. 4. σ^2 (ns^2) obtained from numerical simulations for two different values of the relative phase difference $\Delta\phi_0$, 180° and 245°, respectively, while keeping the other parameters the same. These calculations were carried out under the conditions $f_{\rm m} = 1400$ Hz, $A = 100°$, $r = 0.11$, and $h = 9$. The diffusion process and the final beam size depend sensitively on the value of relative phase difference $\Delta\phi_0$.

chaotic sea of overlapping parametric resonances, the corresponding oscillatory amplitude in σ_t^2 decreases as well. The final equilibrium bunch length is given by the phase space area of the chaotic region.

In conclusion, we have experimentally measured the evolution of a beam distribution as a function of rf parameters in a storage ring. These parameters are the ratio of rf voltages r, the modulation frequency $f_{\rm m}$, the modulation amplitude A, and the relative phase $\Delta\phi_0$. We have found that the evolution of the

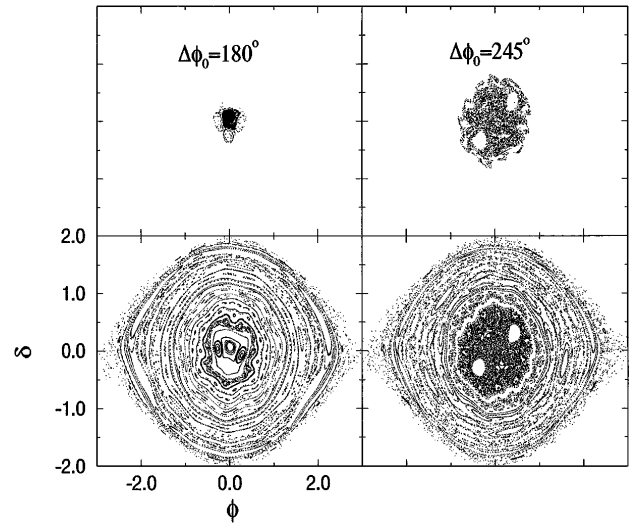

FIG. 5. The Poincaré surfaces of section (bottom plots) and the final beam distribution obtained from numerical simulations (top plots) for two different values of the relative phase difference $\Delta\phi_0$, 180° and 245°. These calculations were carried out under the same conditions as those in Fig. 4. Beam diffusion (or dilution) occurs only when the central region of bucket becomes stochastic.

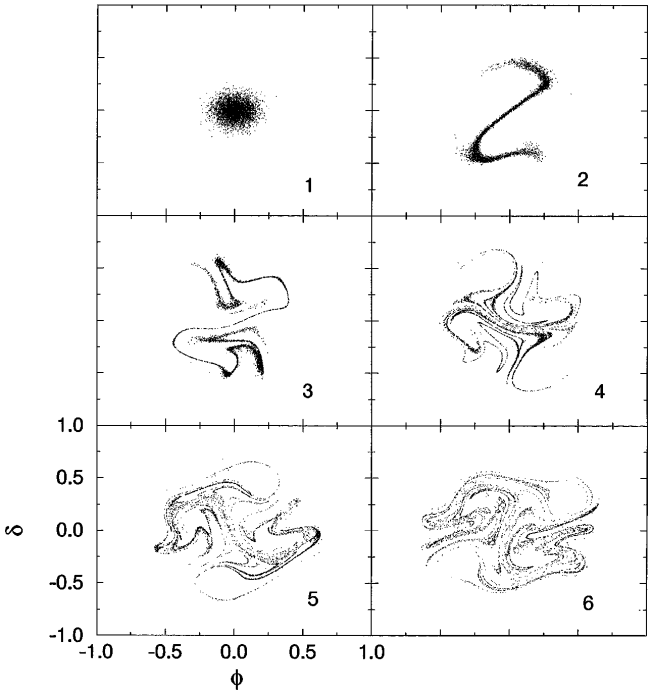

FIG. 6. The time lapse Poincaré surfaces of section show the diffusion process for the parameters $\nu_m = 1400$ Hz, $A = 100°$, $\Delta\phi_0 = 245°$, $r = 0.11$, and $h = 9$. The frames are numbered in chronological orders from 1 to 6 in a time step of 2.92 ms. The fast diffusion process is induced by two overlapping 2:1 parametric resonances, and the slow diffusion process proceeds through the chaotic sea.

bunched beam can be divided into a fast process that is related to particle diffusion along the dominant parametric resonances, and a slow process where particles diffuse inside the chaotic sea.

From our analysis, we find that a linear growth of σ_t^2 with time (see, e.g., the left plot in Fig. 3) can be identified as a diffusion process in a complete chaotic region in the phase space. On the other hand, if the phase space possesses a layer of chaotic sea with invariant tori embedded inside, then σ_t^2 will show characteristics of anomalous diffusion similar to the right plot in Fig. 3. However, if stable islands still exist in the chaotic background as shown in the lower right plot in Fig. 5, the evolution of σ_t^2 will be strongly oscillatory. Our experiments, with numerical simulations, have systematically verified these conditions. The understanding of the signature of the beam phase space evolution can be used to diagnose sources of emittance dilution mechanisms in high brightness beams and space charge dominated beams.

Because of the weak damping of the electron cooling system, the rf phase modulation by a secondary rf system can provide a chaotic dynamical system, where the attractors evolve into nonintersecting attracting lines, which depends sensitively on the value of the damping decrement λ, and the intrinsic diffusion coefficient D. Such systems can also be detected by our beam measurement tools. Employing the sensitivity, values of λ and D can be independently measured.

This work was supported in part by Grant No. DOE-DE-FG02-92ER40747 and Grant No. NSF PHY-9512832.

[1] See, e.g., M. F. Shlesinger, G. M. Zaslavsky, and J. Klaften, Nature (London) **363**, 31 (1993), and references therein.

[2] See, e.g., C. L. Bohn, Phys. Rev. E **50**, 1516 (1994); J. Struckmeier, Phys. Rev. E **54**, 830 (1996), and references therein.

[3] V. V. Balandin, M. D. Dyachkov, and E. N. Shaposhnikova, Part. Accel. **35**, 1 (1991); J. M. Kats, in *Proceedings of the 2nd European Particle Acceleerator Conference* (Edition Frontiére, Gif-sur-Yvette, CEDEX France, 1990), p. 252; J. M. Kats, BNL AGS Technical Notes No. 324, 1989 (unpublished).

[4] High intensity particle beams in synchrotrons can encounter transverse or longitudinal collective instabilities, particularly at the transition energy. Above the transition energy a higher energy particle takes a longer time to complete one revolution than that of the reference particle; it is called a negative mass region. Because all particles isochronously orbit around the synchrotron at the transition energy region, i.e., the synchrotron tune becomes zero, the beam bunch can suffer a collective beam instability called the negative mass instability and lead to uncontrolled beam loss. To minimize the effect of collective beam instability, one usually employs controlled beam manipulation schemes by reducing the line density of the circulating beam, or a faster acceleration rate. Similarly, at low energy, a double rf system has been used to alleviate space charge effects by reducing the peak current of the beam bunch. Since the double rf system increases the synchrotron tune spread of the beam for enhancing Landau damping [8], and changes the time structure of the beam bunch that modifies the effective impedance, it has also been used to overcome multibunch instabilities.

[5] R. Cappi, R. Garoby, and E. N. Shaposhnikova, Report No. CERN/PS 92-40 (RF), 1992; R. Cappi (private communication).

[6] M. Ellison *et al.*, Phys. Rev. Lett. **70**, 591 (1993); H. Huang *et al.*, Phys. Rev. E **48**, 4678 (1993); D. Li *et al.*, Phys. Rev. E **48**, R1638 (1993); D. Li *et al.*, Nucl. Instrum. Methods Phys. Res., Sect. A **364**, 205 (1995).

[7] M. Bai *et al.*, Phys. Rev. E **55**, 3493 (1997).

[8] S. Y. Lee *et al.*, Phys. Rev. E **49**, 5717 (1994); J. Y. Liu *et al.*, Phys. Rev. E **50**, R3349 (1994); J. Y. Liu *et al.*, Part. Accel. **49**, 221 (1995).

[9] See, e.g., S. Y. Lee, in *Accelerator Physics at the SSC*, edited by Y. Yan and M. Syphers, AIP Proc. No. 326 (AIP, New York, 1995), p. 13.